

## Effect of Microwave Irradiation Synthesis of ZnO Nanoparticles

Chelladurai Amutha<sup>1,†</sup>, Balan Natarajan<sup>1,‡</sup>, Sethuramachandran Thanikaikarasan<sup>2,\*</sup>, Adaikalam Cyrac Peter<sup>1</sup>,  
Thaiyan Mahalingam<sup>3</sup>, J. Moreira<sup>4</sup> and P.J. Sebastian<sup>5,‡</sup>

<sup>1</sup>Post Graduate and Research Department of Physics, Raja Dorai Singam Government Arts College,  
Sivagangai - 630 561, Tamil Nadu, India.

<sup>2</sup>Centre for Scientific and Applied Research, School of Basic Engineering and Sciences, PSN College of Engineering and Technology,  
Tirunelveli - 627 152, Tamil Nadu, India.

<sup>3</sup>Department of Electrical and Computer Engineering, Ajou University, Suwon- 443 749, Republic of Korea.

<sup>4</sup>Universidad de Ciencias y Artes de Chiapas, Libramiento Norte Poniente 1150, Tuxtla Gutierrez, 29000, Chiapas, Mexico.

<sup>5</sup>Instituto de Energias Renovables, UNAM, Temixco 62580, Morelos, Mexico.

Received: November 21, 2015, Accepted: December 09, 2015, Available online: January 25, 2016

**Abstract:** Zinc Oxide nanoparticles were synthesized from zinc acetate by microwave irradiation method. X-ray diffraction patterns showed that the prepared samples found to exhibit hexagonal structure. Surface morphology and presence of elements have been analyzed using scanning electron microscopy and energy dispersive analysis by X-rays. The presence of stretching and bending modes in the prepared samples has been determined using Fourier transform infrared spectroscopy. Optical absorption analysis showed that the prepared samples possess band gap value around 3.02 eV. Photoluminescence spectroscopic analysis indicated a strong ultraviolet emission band at 390 nm and a weak blue - green band and weak blue emission band at 484 and 444 nm respectively.

**Keywords:** Microwave synthesis, Nanoparticles, Photoluminescence spectroscopy, Zinc Oxide

### 1. INTRODUCTION

Transparent Conducting Oxides (TCO's) have received much attention due to its wide range of applications in several optoelectronic devices such as light emitting diodes (LED's), solar cells and flat panel displays [1-3]. Indium tin oxide (SnO<sub>2</sub>:In) is the most commonly used TCO for many applications because of its high transmittance in the visible region [4]. Some of the TCO's which have shown transmittance and resistivity values close to the value of SnO<sub>2</sub>: In, SnO<sub>2</sub>: F, TiO<sub>2</sub>: Nb and so on. Among them, zinc oxide (ZnO) is one of the most favourable material because of its kind nature, relatively of low cost, good stability in hydrogen plasma process and non toxicity [4,5]. Consequently, there is considerable interest in understanding the electrical and transparent properties of doped ZnO films, which is critical for further improvement of TCO characteristics. Recently, there is stimulated development of new TCO materials like doped ZnO. ZnO is appeared to be

attractive, because of its various applications in modern devices such as spin-polarized solar cells, magneto optical switches, gas sensors, optical waveguide, flat panel displays and transparent heat mirrors [6-10]. Numerous techniques that have been reported for the preparation of ZnO in the form of films and powders such as RF sputtering [11], magnetron sputtering [12], chemical vapour deposition [13] and sol-gel process [14]. Among them, for some of the techniques there is necessity of high cost equipment and other facilities. Nowadays, microwave energy has become a very efficient means of heating reactions. Chemical reactions that take place over long time to complete can be accomplished in minutes with the aid of microwave radiation [15-16]. Microwave assisted synthesis not only helps in implementing GREEN chemistry but also lead to the revolution in organic synthesis. Microwave irradiation has well known to promote the synthesis of a variety of compounds, where chemical reactions are accelerated because of selective absorption of microwave by polar molecules. ZnO nanostructure with different shapes have been successfully synthesized and

To whom correspondence should be addressed:

\*S\_thanikai@rediffmail.com, †b\_natraj\_b@rediffmail.com, ‡sjp@ier.unam.mx

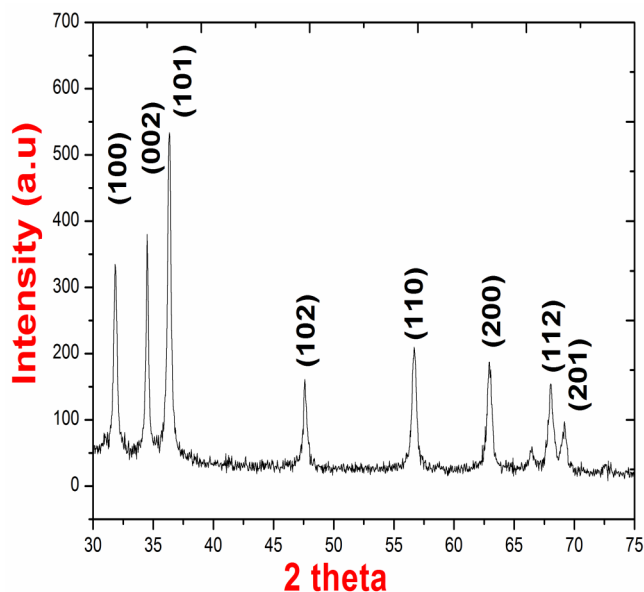


Figure 1. The X-ray diffraction pattern for ZnO nanoparticles synthesized by microwave oven technique.

reported in the literature, such as sharp needle-shaped tetrapods, nanorods, nanowiskers, nanobelts, nanosheets, nanotriangles, nanotubes, nanoprism, nanonails and nanosphere.

For commercial use of ZnO nanostructures, various chemical and physical methods that have been reported for the preparation of the ZnO nanostructures with various sizes and morphologies, which include chemical vapor deposition, physical vapor deposition, vapor phase liquid solid assisted method, chemical solution deposition, pulsed laser deposition, electrochemical deposition, hydrothermal synthesis, microwave assisted synthesis, spray pyrolysis and thermal evaporation. Among them, microwave synthesis is known for homogenous volumetric heating and high reaction rate compared to other physical and chemical methods. In this paper, we have reported an effective method for the preparation of ZnO nanoparticles using microwave irradiation method. Prepared particles were subjected to x-ray diffraction, scanning electron microscopy, UV-Vis-NIR and photoluminescence spectroscopic techniques for structural, morphological and optical properties respectively. The observed results are discussed in detail.

## 2. EXPERIMENTAL

### 2.1. Synthesis of ZnO Nanoparticles

Zinc nitrate tetrahydrate [ $\text{Zn}(\text{NO}_3)_2 \cdot 4\text{H}_2\text{O}$ ], sodium hydroxide (NaOH) and ethanol ( $\text{CH}_3\text{CH}_2\text{COOH}$ ) were used as source materials, purchased from Sigma Aldrich. Zinc acetate [ $\text{Zn}(\text{CH}_3\text{COO})_2$ ] is the chemical compound commonly occurs as  $\text{Zn}(\text{CH}_3\text{COO})_2 \cdot 2\text{H}_2\text{O}$  with molecular weight around 219.49 g/mol. NaOH with molecular weight 39.9971 g/mol was dissolved in water which is strongly exothermic. Water is widely used in chemical reactions as a solvent or reactant and less commonly as a solute or catalyst. In inorganic reactions, water is a common solvent, dissolving many ionic compounds. Millipore water was used as solvent in the preparation of ZnO nanopowder in the present work.

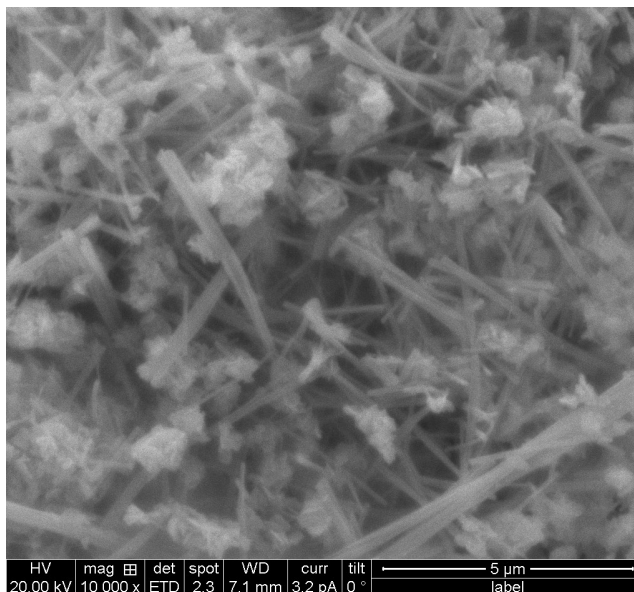


Figure 2. The SEM image for ZnO nanoparticle synthesized by microwave oven technique.

Zinc oxide nanoparticles were prepared by microwave assisted hydrothermal route. 1.6 g of  $\text{Zn}(\text{NO}_3)_2 \cdot 4\text{H}_2\text{O}$  was dissolved in 50 ml deionized water with continuous stirring. 50 ml of 2.2g NaOH solution was added into the solution drop wise followed by stirring process, thus leads to produce aqueous solution with white colour. Thereafter, it was transferred into Teflon-line stainless steel autoclave and the stainless steel autoclave was kept in a silicon carbide chamber. Thereafter it was introduced into microwave irradiation system. Having microwave chamber with 360 x 210 x 430 mm dimension with 2.45 GHz frequency multimode source with maximum deliverable power output of 700 W. The preparation of samples was carried out with different microwave power and irradiation time. The resultant products were in the form of precipitate. The formed precipitate was filtered and washed with distilled water followed by ethanol to remove the ions; the remaining is the white product. Furthermore, the product yield was dried in hot air oven at 80°C. The resultant white product was collected and subjected to characterization.

### 2.2. Characterization

X-ray diffraction pattern of the prepared samples was recorded using X-ray diffractometer (Bruker D8) with  $\text{CuK}_\alpha$  radiation with wavelength ( $\lambda=1.54060 \text{ \AA}$ ). Scanning electron microscope image of all the prepared samples were analyzed using a scanning electron microscope (INPECT-F Model, 30KV). Optical absorption measurements of the prepared samples were measured using a UV-Vis-NIR spectrophotometer (Shimadzu UV-Vis NIR 1800). Photoluminescence spectra of the prepared samples were recorded using a spectro-fluorometer (Perkin Elmer LS55). Fourier transform infrared spectroscopic measurements were carried out using a Shimadzu 8400S FTIR spectrophotometer in the wavenumber range between 400 and 4000  $\text{cm}^{-1}$ .

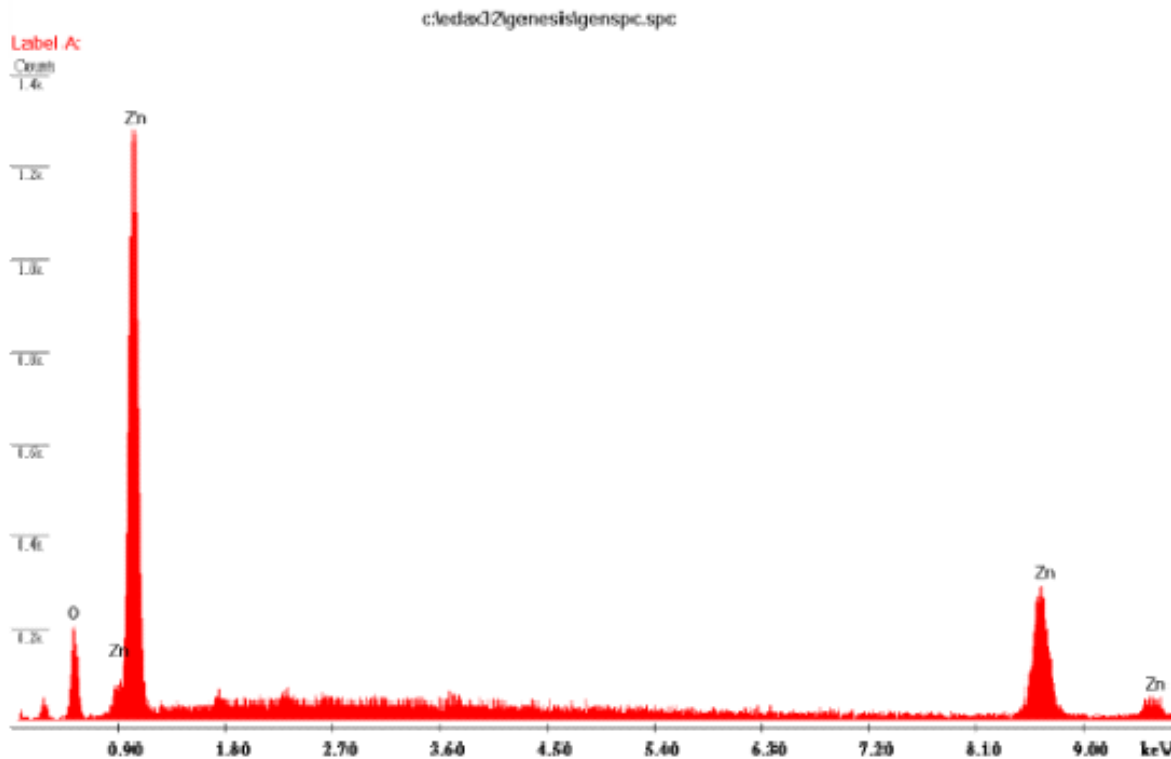


Figure 3. The EDX spectrum for ZnO nanoparticle synthesized by microwave oven technique.

### 3. RESULTS AND DISCUSSION

#### 3.1. Structural Analysis

X-ray diffraction has found many practical applications in nanotechnology. X-ray diffraction (XRD) pattern of the ZnO nanoparticle is shown in Figure 1. It is observed that the diffraction peaks of pure hexagonal ZnO are found at  $2\theta$  values of angles 31.8, 35.36.32, 47.6, 56.7, 62.9, 66.4, 68, 69.14 corresponding to the lattice planes (002), (100), (101), (102), (110), (103), (200), (112) and (201), respectively. The “d” values observed in the present work are in close agreement with JCPDS ICDD file for hexagonal ZnO with lattice parameters ( $a = 3.248 \text{ \AA}$  and  $c = 5.208 \text{ \AA}$ ) [17]. It is also observed that the ZnO nanoparticles have preferential orientation along c-axes, in addition to the fact that the preferential orientation is due to minimization of internal stress and surface energy. The crystallite size is defined as the number of crystallites formed along the plane of the surface. The value of crystallite size is calculated using FWHM data and Debye-Scherrer formula:

$$D = \frac{0.9\lambda}{\beta \cos \theta} \quad (1)$$

where  $D$  is the crystallite size in nm,  $\lambda$  is the wavelength of  $\text{CuK}\alpha$  target used ( $\lambda = 1.54059 \text{ \AA}$ ),  $\beta$  is the full width at half maximum of the peak in radians,  $\theta$  is the Bragg's diffraction angle at peak position in degree. The value of crystallite size for all the samples prepared in the present work is found to be in the range between 30 and 40 nm.

#### 3.2. Morphological and Compositional Analyses

Surface morphology and film composition have been analyzed using energy dispersive analysis by X-rays set up attached with a scanning electron microscope. SEM micrographs clearly indicated the formation of controlled size needle shaped nanoparticles. It is possible to control the size and shape of the synthesized nanoparticles with the help of electron irradiation. SEM picture clearly indicated well-aligned orientation of crystallite with high degree. The grains are in the shape of needles, which is denoted in Figure 2. Typical EDX spectrum of ZnO nanoparticle is shown in Figure 3. The emission lines of Zn and O are present in the investigated energy range indicating the formations of ZnO nanoparticles. The atomic molar ratio (Zn:O) is found to be (47.23:52.77), indicating near stoichiometric nature of ZnO. This result is consistent with X-ray diffraction analysis of the sample with phase corresponding to ZnO.

#### 3.3. Optical absorption analysis

Optical absorption analysis of ZnO nanoparticle has been analyzed using a UV-Vis-NIR spectrophotometer within the wavelength range between 300 and 1200 nm. Room temperature optical absorption spectra of ZnO nanoparticles is shown in Figure 4. It is found that there is observation of broad absorption band at 362 nm corresponding to blue shift compared to the value of bulk ZnO which must be exhibited blue shift at wavelength value around 370 nm. This may be due to presence of quantum confinement effect in the synthesized nanoparticles. This result is in agreement with the value reported earlier by Zhang et al [20]. In this effect, the band

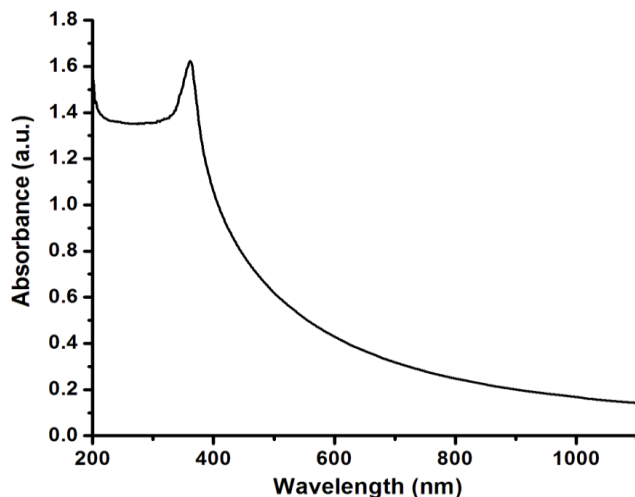


Figure 4. The optical absorption spectra for ZnO nanoparticles synthesized by microwave oven technique.

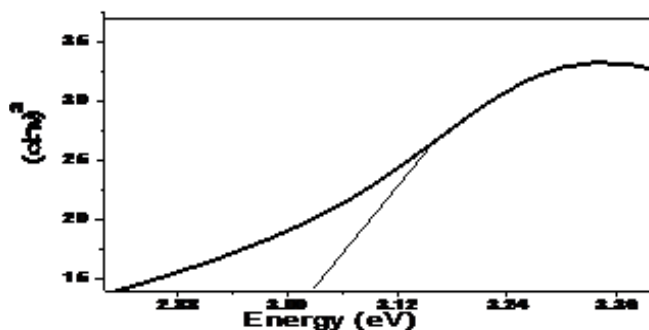


Figure 5. The plots of  $(\alpha hv)^2$  versus  $(hv)$  for ZnO nanoparticles synthesized by microwave oven technique.

gap value of the particle increases resulting shift in the value of absorption edge to lower wavelength leading to produce decrease in value of sizes of the particle. The value of blue shift is large for nanoparticles with small size. In the present work, the value of blue shift is found to be in the range between 8 and 25 nm. This may be due the value of exciton Bohr radius is too small around 2.23 nm which is not comparable to the size of the nanoparticle. The reason for size distribution in one dimensional nanostructure is the effect of quantum confinement depending upon change in width or diameter of the nanoparticles. The nature of transition present in ZnO nanoparticle is determined using the following equation,

$$\alpha hv = K(hv - E_g)^{1/2} \quad (2)$$

where,  $\alpha$  is the absorption co-efficient in  $\text{cm}^{-1}$ ,  $hv$  is the photon energy in eV,  $E_g$  is the band gap value of the materials in eV. A plot of  $(\alpha hv)^2$  versus  $(hv)$  for synthesized ZnO nanoparticle is shown in Figure 5. The linear portion of the graph is extrapolated to X-axis  $(hv)$  giving the band gap value of the material. The band gap value of ZnO nanoparticles obtained in the present work is

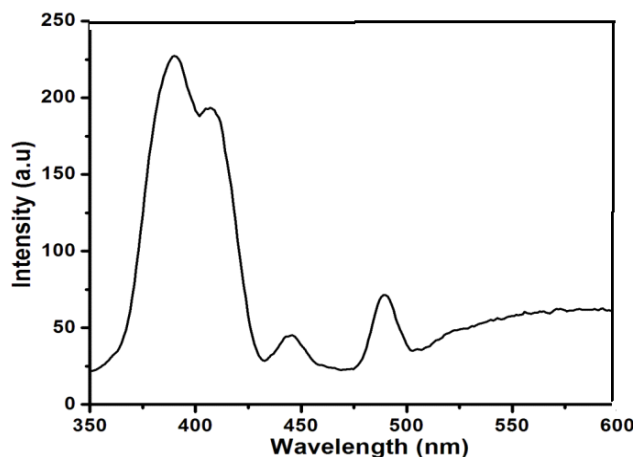


Figure 6. The photoluminescence spectra for ZnO nanoparticles synthesized by microwave oven technique.

found to be 3.02 eV. The band gap value of the material obtained in the present work is found to be in close agreement with the value reported earlier [21]. But, in this case there is an interesting aspect, the observed value of band gap energy of ZnO film is invariably lower than band gap value of bulk ZnO (3.37 eV), which may be due to various lattice associated atomic interaction phenomena come into play from its ionic crystalline lattice nature [22].

### 3.4. Photoluminescence Spectroscopic Analysis

Photoluminescence spectroscopic analyses have attracted many researchers due to its wide range of applications in manufacturing of optical devices. To determine the emissions present in synthesized ZnO nanoparticles, we have carried out Photoluminescence spectroscopic analysis of the synthesized ZnO nanoparticles. Figure 6 shows the photoluminescence spectrum of ZnO nanoparticles. It is observed that the appearance of a peak at 390 nm may corresponds to exciton emission or Ultraviolet emission in ZnO nanoparticles. In the spectral range between 444 and 542 nm it represents emission in visible range corresponding to defect related emission in ZnO nanoparticles. The observation of the peak at 444 nm corresponds to blue band, and the appearance of the peak at 459 nm may be due to the weak blue green band in the wavelength range between 484 and 542 nm. It is also noted that in the region between 444 and 484 nm, there is observation of defects such as interstitial Zn atoms and presence of donor and acceptor states between conduction and valence bands. The appearance of green band results due to the presence of single oxidized oxygen ion vacancy defects in ZnO nanoparticles. As a result the photoluminescence spectrum of ZnO nanoparticles consists of narrow ultraviolet region accompanied by strong visible emission when a sample is excited by a xenon lamp at 225 nm. The smaller size nanoparticles exhibit strong visible emission due to the presence of large number of surface defects. This may be due to high surface to volume ratio of ZnO nanoparticle as size of the particle decreases. As a result, large number of defects are found on the surface. The process of surface modification of ZnO nanoparticles results in suppression of the region facilitating ultraviolet emission. The sample exhibited

room temperature photoluminescence spectra showing strong ultraviolet emission band at 390 nm, weak blue green band at 484 nm and very weak blue band at 444 nm, respectively. The observation of strong ultraviolet emission band at 390 nm may be attributed to band-edge exciton transition in the synthesized nanoparticles. The appearance of peaks at 444 nm and 484 nm are much weaker. The emission peak at 444 nm may originate from the electron transition from the interstitial atom of Zn ( $Zn_i$ ) defect energy level to  $V_{Zn}$  defect energy level, and the peak at 484 nm is due to the electron transitions from the bottom of the conduction band to the  $O_{Zn}$  defect level. This observation is in close agreement with the results reported by Ding et al [24]. The band gap value of ZnO nanoparticles is determined from photoluminescence spectra using the following equation,

$$E_g = \frac{hc}{\lambda} \quad (3)$$

where,  $E_g$  is the band gap value of the material,  $h$  is the Planck's constant,  $c$  is the velocity of light and  $\lambda$  is the wavelength of photoluminescent emission. The band gap for ZnO nanoparticles was found to be 3.05 eV.

### 3.4. Vibrational Spectroscopic Analysis

Fourier transform infrared spectra have been taken to find out the presence of elemental constituents, chemisorbed species and various functional groups present in the material. It also provides information about the presences of incoming and outgoing species or impurities that may exist near the surface of ZnO nanoparticles. Transmittance is the main characteristic of Zn-O vibration in FTIR spectra and depends mainly on the morphology of ZnO nanoparticles. The series of absorption peaks are presented in the wave number range between 400 to 4000  $cm^{-1}$ , which corresponds to existence of functional groups in the ZnO nanoparticles. A series of absorption peaks are observed corresponding to the presence of different impurities such as hydroxyl, alkane and carboxylate groups in vibration mode. The hydroxyl impurity groups result from hydroscopic character of ZnO nanoparticles. The carboxylate group results from reactive carbon containing plasma species during the formation of ZnO nanoparticles. The FTIR spectrum of ZnO nanoparticles is shown in Figure 7. The appearance of the peak at 485  $cm^{-1}$  indicates the presence of Zn-O stretching mode frequency of ZnO nanoparticle. The peaks observed at 1415 and 1560  $cm^{-1}$  correspond to C = O and O – H bending vibrations, respectively. It is also observed that the peaks at 3422 and 2065  $cm^{-1}$  indicate the presence of – OH and C = O residues, probably due to atmospheric moisture and CO<sub>2</sub> respectively. The appearance of the band in the wave number range between 3200 and 3600  $cm^{-1}$  may correspond to stretching vibration of – OH bond and the peak at 1638  $cm^{-1}$  appears just at half of 3200  $cm^{-1}$ , which has been assigned to the first overtone of the fundamental stretching mode of – OH. These stretching vibrations correspond to water molecule bound on the sample surface. The observed results are in accordance with the data reported earlier by Ziaul et al [23].

### 4. CONCLUSIONS

Zinc oxide nanoparticles were successfully synthesized by microwave oven technique. X-ray diffraction pattern showed that the

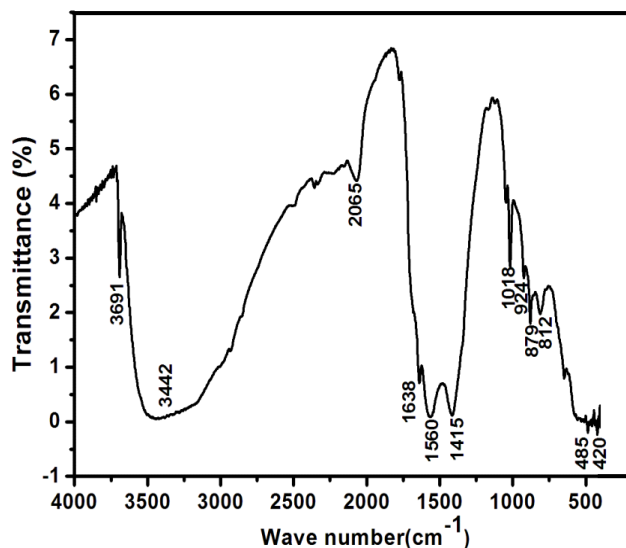


Figure 7. The FTIR spectra for ZnO nanoparticles synthesized by microwave oven technique.

prepared samples exhibited Wurtzite structure with preferential orientation along (002) plane. Scanning electron microscope images indicated the formation of nanoparticles with needle shaped grains. Optical absorption analysis showed that the prepared nanoparticles exhibited a blue shift at a wavelength of 362 nm due to quantum confinement effect when compared to that of bulk ZnO having wavelength value around 370 nm. FTIR analysis indicated the presence of Zn-O stretching mode at wave number value around 485  $cm^{-1}$ . Photoluminescence spectroscopic analysis revealed that there was appearance of strong ultraviolet emission peak centered at 390 nm corresponding to a weak blue-green band, appearance of peak at 484 nm corresponds to a very weak blue band and appearance of the peak at ~444 nm indicated the appearance of a very weak blue band which denoted that the prepared sample exhibited better crystallinity.

### 5. ACKNOWLEDGEMENTS

This work was partially supported by the grants PAPIIT IT100413 and CONACYT 236978.

### REFERENCES

- [1] J. Lee, J. Metson, P.J. Evans, R. Kinsey, D. Bhattacharyya, *Appl. Surf. Sci.*, 253, 4317 (2007).
- [2] G. Akhlesh, A.D. Compaan, *Appl. Phys. Lett.*, 85, 684 (2004).
- [3] O. Bamiduro, H. Mundle, R.B. Konda, A.K. Pradhan, *Appl. Phys. Lett.*, 90, 252108 (2007).
- [4] V. Bhosle, A. Tiwari, J. Narayan, *J. Appl. Phys.*, 100, 033713 (2006).
- [5] A. Ashour, M.A. Kaid, N.Z. El-Sayed, A.A. Ibrahim, *Appl. Surf. Sci.*, 252, 7844 (2006).
- [6] M.R. Vaezi and S.K. Sadmezhad, *Materials and Design*, 28, 515 (2007).
- [7] Y.J. Kwon, K.H. Kim, C.S. Lim, and K.B. Shim, *Journal of*

- Ceramic Processing Research, 3, 146 (2002).
- [8] J.G. Lu, Z.Z. Ye, J.Y. Huang, L.P. Zhu, and B.H. Zhao, *Applied Physics Letters*, 88, 063110 (2006)
- [9] A.D. Yoffe, *Advances in Physics*, 51, 799 (2002).
- [10] N.F. Hamedani and F. Farzaneh, *Journal of Science: Islamic Republic of Iran*, 17, 231 (2006).
- [11] Z. Hu, G. Oskam, and P. C. Searson, *Journal of Colloid and Interface Science*, 263, 454 (2003).
- [12] B. D. Cullity, *Elements of X-Ray Diffraction*, Edition-Wesley, Reading, Mass, USA, (1978).
- [13] G. Glaspell, P. Dutta, and A. Manivannan, *Journal of Cluster Science*, 16, 523 (2005).
- [14] N.V. Tuyen, N.N. Long, T.T.Q. Hoa, T.D. Canh, *Journal of Experimental Nanoscience*, 4, 243 (2009).
- [15] M. Kooti and A. Naghdi Sedeh, *Journal of Chemistry*, Article ID: 562028 (2013).
- [16] B.D. Cullity, *Elements of X-ray Diffraction*, Addison-Wesley, Reading, Massachusetts, 356 (1979).
- [17] N. Faal Hamedani and F. Farzaneh, *Journal of Sciences: Islamic Republic of Iran*, 17, 231 (2006).
- [18] S. Thanikaikarasan, K. Sundaram, T. Mahalingam, A. Kathalingam, *Jin-Koo Rhee, Vacuum*, 83, 1066 (2009).
- [19] B.D. Cullity, *Elements of X-ray diffraction*, 2nd Edition, Addison- Wesley Publishing House, Massachusetts, USA, 1969.
- [20] H. Zhang, D. Yang, S. Li, X. Ma, Y. Ji, J. Xu, D. Que, *Mater. Lett.*, 59, 1696 (2005).
- [21] L.C. Nehru, M. Umadevi, C. Sanjeeviraja, *International Journal of Materials Engineering*, 2, 12 (2012)
- [22] J. Gonioakowski, C. Noguera, *Surf. Sci.*, 340, 191 (1995).
- [23] Ziaul Raza Khan, *Material Science and Applied Physics*, 2, 340 (2011).
- [24] W.M. Huang, B. Yang, Y. Zhao, Z. Ding, *Mater. Lett.*, 62, 498 (2008).